

Electrochemical Determination of the Free Energy of Formation of Tantalum Oxide

GIOVANNI B. BARBI

High Temperature Chemistry Group, EURATOM CCR Ispra
Ispra (Italy)

(Z. Naturforsch. 25 a, 1515—1516 [1970]; received 11 May 1970)

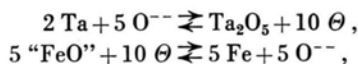
As it has been demonstrated by many authors, the determination of the thermodynamic stability of metal-oxygen systems may be performed by electromotive force measurements across all-solid galvanic chains¹. The electrolyte, consisting of a highly defective solid solution of refractory oxides, must exhibit a pure ionic conductivity in order to avoid the establishment of both junction potentials and irreversible polarization phenomena.

The cell under investigation was:

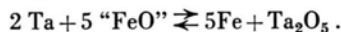
Pt | Ta + Ta₂O₅ | ThO₂ (+15 Mol.% La₂O₃) | Fe + "FeO" | Pt
"FeO" indicating the iron-defective, iron monoxide-wüstite phase in equilibrium with iron.

Provided that the above-mentioned condition be satisfied, the e.m.f. developed at the ends of this cell yields directly, by means of the basic Nernst relationship, the difference between the partial molar free energies of oxygen in equilibrium with the electrode systems.

The virtual electrochemical reactions are:



and the total process is:



Neglecting the solubility of oxygen in the metal phases, i. e. considering the metal phases as pure phases, it is possible to write:

$$\mu_{\text{O}_2, \text{Ta}_2\text{O}_5} - \mu_{\text{O}_2, \text{"FeO"}} = \frac{2}{5} \Delta G_{f, \text{Ta}_2\text{O}_5}^0 - 2 \Delta G_{f, \text{"FeO"}}^0 = -4 F E \quad (1)$$

where μ_{O_2} 's are the partial free energies (Gibbs potentials) of oxygen in equilibrium with metal + metal oxide systems, $\Delta G_{f, \text{Ta}_2\text{O}_5}^0$ the standard molar free energy of formation from the elements of Ta₂O₅, $\Delta G_{f, \text{"FeO"}}^0$ the standard free energy of formation of wüstite per atom of oxygen and E the e.m.f. values, as measured from the right to the left.

The solid components of the galvanic chain are pellets of 12 mm diameter and 3–4 mm thick. They were laid one upon the other in an alumina crucible, placed in a silica tube, as shown in a previous work². Around the crucible a sheet of zirconium was wound in order to getter the residual oxygen surrounding the cell. The

measuring and recording apparatus was described previously².

The iron + iron oxide pellets were prepared by thoroughly blending very fine powders of Fe and Fe₂O₃ in such a ratio as to get a final composition of about 25 at.-% of oxygen, pressing in a die and then annealing overnight under vacuum at 1000 °C. Analogously, tantalum + tantalum oxide pellets were sintered after blending extremely fine (25 000 mesh/cm²) component powders in such a ratio as to get a 20 at.-% oxygen composition. The preparation of the intermediate electrolyte pellets was described elsewhere³.

The experimental results are reported in the following table:

	Run No.	<i>T</i> (°K)	<i>E</i> (mV)
Cell No. 1	1	1275	585,2
	2	1276	586,8
	3	1221	592,2
	4	1183	596,3
	5	1125	600,5
	6	1079	607,7
	7	1098	604,5
	8	1153	598,7
	9	1188	594,7
	10	1241	586,6
	11	1210	591,5
	12	1168	596,7
Cell No. 2	13	1272	585,9
	14	1080	605,2
Cell No. 3	15	1232	587,1

Table 1.

The results are reproducible and the e.m.f. values are stable over many hours. The complete stabilization of the e.m.f. after changing the running temperature takes a time ranging between 10' and one hour, depending on the temperature itself. Run No. 1 of cell No. 1 was obtained with a non-stationary technique after polarization, a technique developed by the author some years ago⁴. During this run the residual oxygen pressure in the cell was higher than the oxygen pressures of the other runs because the zirconium getter was not placed into the cell. Anyway the e.m.f. value is comparable with the others since the equivalence of the stationary and the non-stationary methods has been demonstrated².

The E vs. T function has been approximated by a straight line (reported in Fig. 1), and the following equation has been calculated using the least squares method:

$$E(\text{mV}) = 723,6 - 0,1087 T(^{\circ}\text{K}). \quad (2)$$

The standard deviation results as ± 1.27 mV.

¹ An exhaustive review of the entire subject has been done by B. C. H. STEELE, Proc. Symp. Nuffield Res. Group, Imperial College London 1967 (Publ. by the Inst. of Mining and Metallurgy).

² G. B. BARBI, Z. Naturforsch. 23 a, 800 [1968].

³ G. B. BARBI, Z. Naturforsch. 24 a, 1580 [1969].

⁴ G. B. BARBI, Trans. Faraday Soc. 62, 1589 [1966].

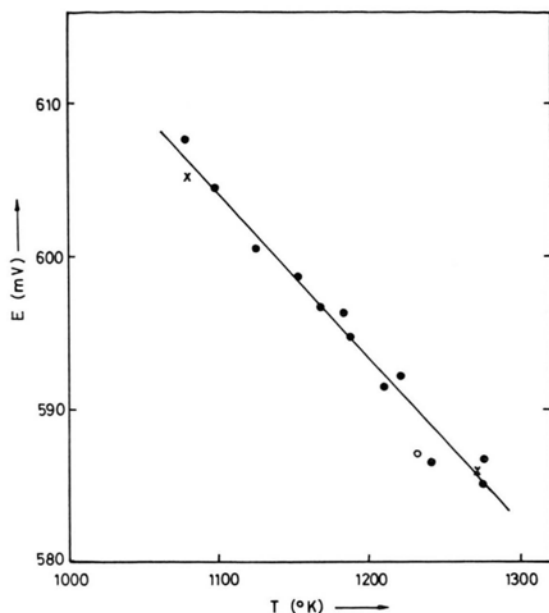
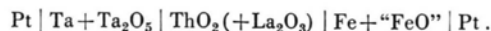


Fig. 1. Electromotive force vs. temperature of the electrochemical cell:



The recently reported JANAF data⁵ have been taken into account for calculating the $\Delta G_{f,\text{"FeO"}}^0$ vs. T function. This function, in the range 1000–1300 °K, may be fairly well approximated by the linear relationship:

$$\Delta G_{f,\text{"FeO"}}^0 = -63.25 + 15.56 \cdot 10^{-3} T \text{ kcal/atom of oxygen.} \quad (3)$$

Substituting Equations (2) and (3) in Eq. (1), yields ($F = 23.06 \text{ kcal} \cdot \text{Volt}^{-1} \cdot \text{equiv.}^{-1}$):

$$\frac{\Delta G_{f,\text{Ta}_2\text{O}_5}^0}{5} = -96.62 + 20.57 \cdot 10^{-3} T \text{ kcal/atom of oxygen.}$$

⁵ JANAF Thermochemical Tables Addendum PB 168 370/1 (Clearinghouse 1966).

The Temperature Dependence of Far Infra-red Absorptions in Non-polar Liquids

B. PETERMAN, B. BORŠNIK, and A. AŽMAN

Department of Chemistry, University of Ljubljana
and Chemical Institute Boris Kidrič
Ljubljana, Yugoslavia

(Z. Naturforsch. **25 a**, 1516–1517 [1970]; received 3 June 1970)

Recent measurements¹ of non-polar liquids in the far infra-red have confirmed the expectations of POLEY² and WHIFFEN³ by showing the presence of a distinct absorption. The possible origins of the absorption have already been discussed^{4,5}. To add some new data we have measured the temperature dependence of the infrared absorption in the range 10–100 cm^{-1} for three non-polar liquids: C_6H_6 , CS_2 and CCl_4 .

All spectra were recorded on a Fourier spectrophotometer with a RIIC variable temperature cell.

The three characteristic features of the measurements are (Figs. 1–3 and Table 1):

1. The ratios of the integrated absorption intensities of $\text{C}_6\text{H}_6 : \text{CS}_2 : \text{CCl}_4$ are 1 : 0.75 : 0.36.
2. There is an increase of the integrated absorption intensity with the decrease of temperature.
3. The bands shift to higher frequencies with increasing temperature.

The integrated absorption intensities depend on the moments of inertia and the observed trend suggests the rotational origin of these bands. This statement has to

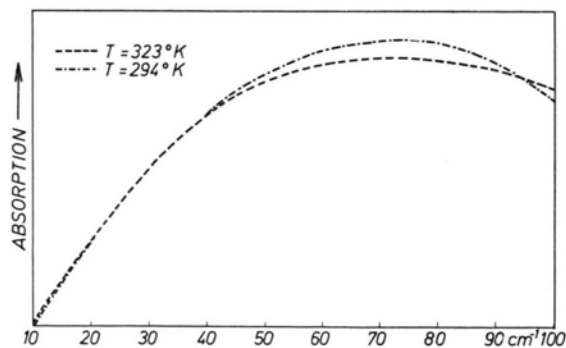


Fig. 1. The effect of the temperature on the absorption of C_6H_6 .

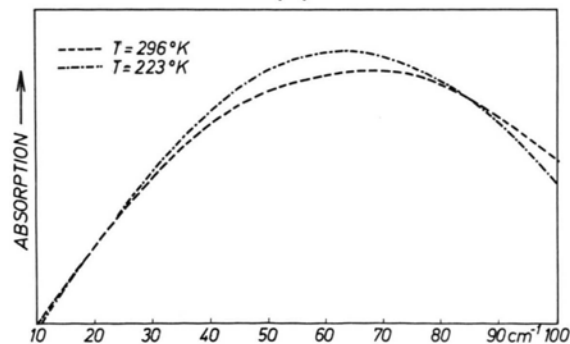


Fig. 2. The effect of the temperature on the absorption of CS_2 .

¹ S. K. GARG, J. E. BERTIE, H. KLIP, and C. P. SMYTH, J. Chem. Phys. **49**, 2551 [1968] and references therein.

² J. PH. POLEY, J. Appl. Sci. B **4**, 337 [1955].

³ D. H. WHIFFEN, Trans. Faraday Soc. **45**, 124 [1949].

⁴ N. E. HILL, Chem. Phys. Letters **2**, 5 [1968].

⁵ J. CHAMBERLAIN, Chem. Phys. Letters **2**, 464 [1968].

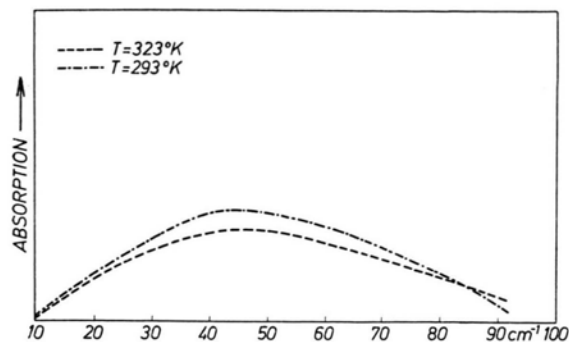


Fig. 3. The effect of the temperature on the absorption of CCl_4 .

	Temperature interval (T in $^{\circ}\text{C}$)	I.A. 1 (%)	B.S. (cm^{-1})
C_6H_6	27	4	2
CS_2	70	5	5
CCl_4	35	7	4

Table 1. The observed changes of the integrated absorption intensity (I.A. 1) and band shifts (B.S.).

be taken with caution because the moment analysis of bands may show that the calculated moments of inertia have not the same trend as the moments calculated from the geometry of the molecules.

The increase of the integrated absorption intensity with decreasing temperature is small but nevertheless only a part of this increase can be accounted for by the larger band width at higher temperature. This observation can be qualitatively explained by the assumption⁶ that the absorption is not due to isolated molecules but is a result of the collective behaviour of the liquid.

The increase in half-width of the bands at higher temperatures supports the assumption that the absorption is of the resonance character. The temperature dependence of the band shift emphasizes the translational⁷ character of the absorption.

The observed changes cannot be explained using the measurements in Ref. ¹ with the assumption that only Debye relaxation absorption (below 10 cm^{-1}) is responsible for the observed changes.

Our measurements are consistent with the proposition^{4,5} that the absorption is of the resonance character with rotation-translation mechanism where the collective behaviour of the liquid is an important factor⁶.

The authors are grateful to the Beckman-RIIC limited for making Fourier Spectrophotometer F 720 available to us.

⁶ H. S. GABELNICK and H. L. STRASS, *J. Chem. Phys.* **49**, 2334 [1968].

⁷ D. R. BOSOMWORTH and H. P. GUSH, *Can. J. Phys.* **43**, 751 [1965].

The Effect of Carrier Concentration on Microwave Emission from n-Type Indium Antimonide

W. A. PORTER and D. K. FERRY

Department of Electrical Engineering, Texas Tech University
Lubbock

(*Z. Naturforsch.* **25 a**, 1517–1518 [1970]; received 27 July 1970)

The effect of carrier concentration on the threshold for microwave emission from InSb was determined. Threshold electric fields are lower for higher concentrations and the magnetic field dependence is reduced.

The influence of carrier concentration on the threshold values of the applied electric and magnetic fields required to stimulate microwave emission was determined by using otherwise similar samples in identical experiments. The power gain for samples of different carrier concentration was determined by comparing the percent change in applied electric field strength required to increase emission from the threshold level to an arbitrary higher level. Also the effect of diffused n^+ contacts on microwave thresholds was studied by first diffusing Sn to a depth of $30\text{ }\mu$ and then removing this layer in stages and comparing the resulting threshold curves.

The samples used had carrier concentrations of $2 \times 10^{14}/\text{cm}^3$, $3 \times 10^{15}/\text{cm}^3$, and $1.9 \times 10^{16}/\text{cm}^3$ and mobilities of $6.5 \times 10^5\text{ cm}^2/\text{V-sec}$, $2.2 \times 10^5\text{ cm}^2/\text{V-sec}$, and $1.2 \times 10^5\text{ cm}^2/\text{V-sec}$, respectively. The InSb was cut into $.5 \times .5 \times 5.0\text{ mm}^3$ bars and then polished in CP4. Ohmic contacts were applied using Sn and a ZnCl_2 flux. The samples were cooled to 77°K in liquid nitrogen. The electric field was supplied in $10\text{ }\mu\text{sec}$ pulses and the perpendicular magnetic field by a 0–6 kG electromagnet. A heterodyne microwave receiver with a sensitivity of -95 dBm tuned to 2 GHz detected the emission which had first been passed through a high pass filter to limit spurious signals. The output of this receiver was displayed on an oscilloscope.

For the lowest carrier concentration, the threshold for emission was similar to that reported earlier¹, the required electric field increasing sharply as the magnetic field was decreased as shown in Fig. 1. Samples of the intermediate concentration behaved quite differently with the required electric field being approximately constant at 12 V/cm and emission persisting as B was reduced toward zero. For the highest concentration, the required electric field strength was only 3 V/cm .

¹ D. K. FERRY and W. A. PORTER, *Microwave Emission and High Frequency Oscillations in n-Type InSb*, *IBM Journal* **13**, 621 [1969].

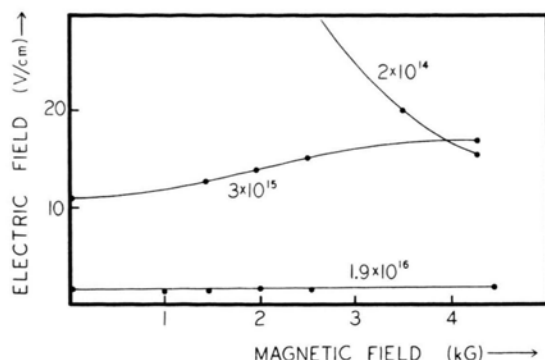


Fig. 1. Microwave emission threshold curves for different concentration samples.

Again the magnetic field had essentially no effect on the threshold electric field. It is evident that the influence of the magnetic field decreases with increase in carrier concentration and that emission from samples of the highest concentration show a virtual independence of the magnetic field.

When the electric field required for an arbitrary emission level is compared with that required for the

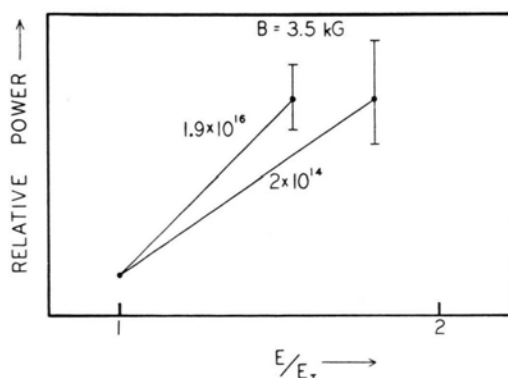


Fig. 2. Power gain for different concentration samples.

initiation of emission at a fixed magnetic field strength, the power gain for a sample can be determined. Shown in Fig. 2 are data for samples of the different concentrations, where the applied electric field has been normalized to threshold electric field value (E_t). It can be seen that the samples of higher carrier concentration exhibit a larger power gain for $B = 3.5$ kG. That is, the same arbitrary power level was reached for a lower normalized electric field. At higher magnetic fields (e. g. 4.6 kG) all concentrations had approximately the same gain.

Tin was diffused into the contact area of some samples ($n = 2.5 \times 10^{14} \text{ cm}^{-3}$) to a depth of 30μ to form $n+$ diffused contacts. The threshold for microwave emission was determined as the diffused layer was etched away in stages by dilute CP4. For low etch times, in which very little of the contact is removed, the threshold is similar to that observed for the highest concentration samples used above. For longer etch times (70 sec) the threshold increased and approached that observed for samples of the lowest concentration, i. e. the concentration of the bulk material.

Several mechanisms have been advanced as explanations of the microwave emission. Effects in the contact region are frequently mentioned and the data reported here tend to confirm this. The results of the contact studies would indicate that the emission is beginning in the high concentration contact regions at a lower threshold than the bulk, so that the emission is dominant in the contact region. We do not feel, however, that field constriction near the contact², is the key mechanism, particularly since the threshold appears relatively independent of magnetic field at higher carrier concentrations. If field constriction were the cause, samples with n -plus diffused contacts would be expected to exhibit higher, rather than lower, emission thresholds since lower electric field gradients would result at the contacts.

² A. H. THOMPSON and G. S. KINO, Noise Emission from InSb, IBM Journal 13, 616 [1969].